Optica Applicata, Vol. LV, No. 3, 2025
DOI: 10.37190/oa/208834

Research on target state recognition algorithm for fiber optic sensing network based on data mining

CHUNHANG QU[1], DAJUN CHANG[2,*], JIAN HU[3]

[1] College of Computer Science, Changchun Humanities and Sciences College, Changchun 130607, Jilin, China

[2] School of Railway Locomotive and Rolling Stock, Jilin Tiedao University, Jilin 132299, Jilin, China

[3] Equipment Department, FAW-FINDREAMS New Energy Technology Limited Company, Changchun 130000, Jilin, China

To obtain the state information of multiple targets in a fiber optic sensing network, we improve the target state recognition probability. A target state recognition algorithm based on data mining is proposed. An orthogonally distributed FBG sensing network is designed based on the characteristics of fiber optic sensing. The clustering weights and clustering degree for multi-target state classification are derived. A target state recognition model based on data mining is constructed. The time interval between peak-to-peak tip positions in an aliased signal containing a faster-moving target is narrower. The more targets are aliased, the greater the time width of the overall echo response. The average test speeds for target A, target B, and target C are 0.99 m/s, 2.86 m/s, and 4.87 m/s, with relative errors of 1.3%, 4.7%, and 2.5%, respectively. The experimental comparison of target recognition probabilities before and after data mining shows that the recognition rate is significantly improved after applying this algorithm. It is especially effective for overlapping signals of state-similar targets. Moreover, this algorithm also suppresses the system's false judgment rate to a certain extent.

Keywords: fiber optic sensor networks, data mining, FBG distribution design,clustering algorithm.

1. Introduction

Fiber optic sensing technology is widely used in fields such as large-scale security, regional target localization, and identification due to its characteristics of broad testing range and high sensitivity [1-3]. With the increase in the testing area and the number of targets within the testing range, signal aliasing leads to a higher false detection rate. It becomes a major challenge in target recognition and state analysis. Improving data recognition rates has become a research focus in the state recognition of targets in fiber optic sensing networks.

TEJEDOR *et al*. [4] laid out a fiber optic sensing network along a pipeline to capture surrounding vibration signals, thereby determining whether there is engineering activ-

ity that may harm the pipeline, enabling classification of different interference signals. SIDELNIKOV *et al*. [5] tested several abnormal interference sources and analyzed them based on the frequency comparison results. The detection rate could reach 87.4%, but could not analyze the motion state of the targets. LI *et al*. [6] used neural networks to analyze construction vibration data. The test position of the target can be inverted with an accuracy of ±5 m. LIU *et al*. [7] combined deep learning and genetic algorithms to enhance the signal-to-noise ratio of target signals in fiber optic sensing data. Compared to the amplitude recognition method, its recognition rate was improved by 45%. GENG *et al*. [8] designed an information entropy-based feature separation algorithm. It was used to test the anomalous nodes in fiber optic sensing networks, achieving an accuracy superior to 93.4%. However, it could only recognize the characteristic anomalies. CHE *et al*. [9] applied an algorithm combining sliding window and confidence. It compares two types of noise for interference target recognition, improving the fault tolerance of target identification. LIANG *et al*. [10] designed an adaptive algorithm for fiber optic sensing networks. The correlation coefficient is better than 0.92 for the 2 kinds of anomalous signals to be recognized. PAN *et al*. [11] used multiple fiber grating sensors to acquire target vibration signals. The classification accuracy can reach 93.3%. When the number of FBGs exceeds 30, the signal differentiation will decrease significantly. SHANG *et al*. [12] integrated variational mode decomposition with support vector machines to identify four types of abnormal signals, achieving an accuracy greater than 98.4%. The existing literature mainly judges whether the target exists and its type, while there is relatively little analysis on the motion state of multiple targets. This article focuses on the design of FBG sensor distribution to achieve simultaneous recognition of multiple targets and states.

Artificial neural networks [5], genetic algorithms [7], data mining [8], *etc*., have their own scope of application. Although artificial neural networks have better learning ability, they are prone to falling into local optima when the data volume is large [9]. Genetic algorithms can achieve multi-target type comparison, which is conducive to multi-parameter optimization. However, it requires a large amount of data to complete the a priori parameter setting and is prone to large deviations when unknown targets enter the network. The advantage of data mining is that it can be used for fast processing of large amounts of data with low dependence on a priori parameters. In contrast, due to the orthogonal setting of FBG positions in this system, there is a certain correspondence between test data and test positions, which reduces the requirements for data processing. This algorithm constructs an input layer set that conforms to the data type based on data features, and then uses data mining algorithms to complete classification, thereby improving the probability and speed of target state recognition.

2. FBG distribution design and target state recognition

In the testing range of the fiber optic sensing network, the echo signals from the targets exhibit different characteristics under various states. Classifying the features of the

original data based on signal characteristics is of great significance for target state inversion [13]. The state parameters of the target mainly include: position and velocity. Let the position of the target be (x_i, y_i), and the velocity be v. The FBG closest to the target produces the strongest echo response, and the coordinate position of the target can be calculated based on the degree of response of the FBG. We have designed an orthogonal arrangement where one horizontal FBG sensor is followed by one vertical FBG sensor, arranged alternately. The location of the numbering of these FBG sensors is known. This design aims to have universality of test results within a larger testing scope. The velocity of the target can be calculated based on the time between different FBG positions of the target. Let the initial wavelength of the FBG sensor be λ_B. When the target affects the FBG, the relationship between the wavelength change and the initial wavelength is as follows:

$$\Delta\lambda_B = \lambda_B\left[(\alpha+\xi)\Delta T + (1-P_e)\Delta\varepsilon\right] \tag{1}$$

Among them, $\Delta\lambda_B$ is the wavelength variation of FBG, α is the thermal expansion coefficient of FBG, ξ is the thermo-optical coefficient of FBG. ΔT is the temperature variation. P_e is the elastic optical coefficient of FBG. $\Delta\varepsilon$ is the axial strain of FBG. Since the target motion speed is much larger than the ambient temperature change speed, Eq. (1) can be simplified as

$$\Delta\lambda_B = \lambda_B(1-P_e)\Delta\varepsilon + c_t \tag{2}$$

where c_t is the temperature compensation coefficient. In the test area, the FBG sensors are laid out as shown in Fig. 1.

From time t_1 to time t_2, the target moves from P_1 to P_2. When the sampling interval is Δt, the response signal of FBG_i is

$$\Delta\lambda_{\mathrm{FBG}_i} = \lambda_{\mathrm{FBG}_i}(1-P_e)\Delta\varepsilon_i(x_1, y_1, t_1, \Delta t) + c_t \tag{3}$$

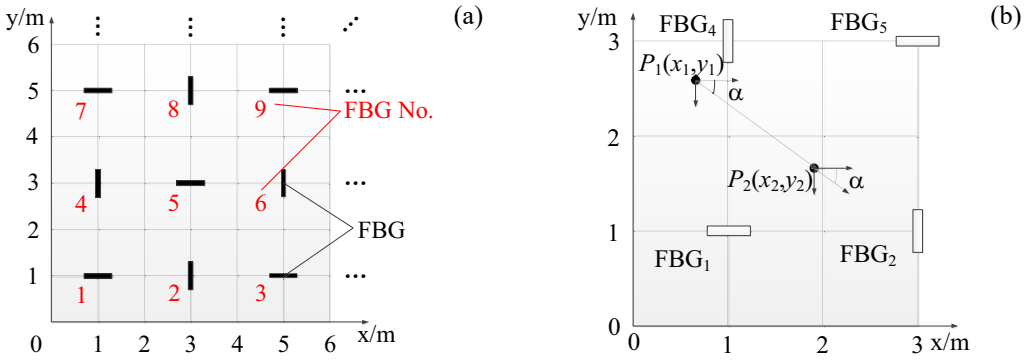

Fig. 1. Distribution design of FBG sensors in fiber optic sensing network. (a) FBG distribution. (b) Position changes of target in the testing area.

The target velocity v can be expressed as

$$v = \frac{\sqrt{(x_2 - x_1)^2 + (y_2 - y_1)^2}}{t_2 - t_1} \tag{4}$$

The target position (x_2, y_2) can be represented as

$$\begin{cases} (x_2, y_2) = (x_1 + v\sin\alpha\Delta t, y_1 + v\cos\alpha\Delta t) \\ \alpha = \arctan\dfrac{y_2 - y_1}{x_2 - x_1} \end{cases} \tag{5}$$

The state of the target can be obtained by Eqs. (4) and (5). The time can be calculated from the clock of the test system. Parameters can be calculated from the calibration when the state is known. The coordinate position can be calculated from Eq. (3) by testing the wavelength variation. The placement depth of FBG will have an impact on the test results, so in order to obtain better response, the FBG sensor is placed at a depth of about 2 mm. This depth is sufficient to protect the integrity of the FBG sensor while still maintaining good sensitivity.

3. Design of target state recognition model

3.1. Data mining and classification

For a single target, its correct rate is high. But when there are multiple targets, especially when the motion areas of the targets are close to each other. The response signals of FBG will have the problem of aliasing. This phenomenon will significantly reduce the target recognition probability. To improve the recognition probability of target states, multi-target echo signals are classified and recognized by data mining. For the data classification problem, cluster analysis is a commonly used data mining tool. The essence of cluster analysis is to categorize similar data together and build a similarity matrix about the data types based on the data features. Thus, the mapping relationship between the original data and the data to be processed is accomplished.

Let the weight of the target be tested and the set of all wavelength responses be $c_m(t_i)$, t_i is the time, m is the serial number of the FBG at the test point, and $m = 1, 2, ..., M$. The clustering weights are calculated by categorizing the sampled data from t_1 to t_i:

$$c_m(t) = \sum_{m=1}^{M} \mu_m c_m(t-1) \tag{6}$$

where μ_m is the fuzzy affiliation degree, $1 \le m \le M$. Let the information set $A = = (a_1, a_2, ..., a_n)$ of the target to be measured contain the density metrics that characterize its state:

$$D_i = \sum_{m=1}^{M} \exp\left\{-\frac{4}{\mu_m^2}\left[c_m(t) - c_{m-1}(t)\right]^2\right\} \tag{7}$$

When the density in the region reaches a maximum value of $c_{\max}$, the density metric of the target state information is $D_{\max}$. The ratio of the density metric D_i to the maximum value of $D_{\max}$ ($f_i = D_i/D_{\max}$) is applied to determine whether the test point is the same class of target data. The ratio is affected by the target state information weights and the radius of the neighborhood at the corresponding location. The smaller its ratio, the more effective the clustering algorithm is in clustering the initial data. The higher the relevance of its data, the easier it is to improve the target recognition probability. Then the clustering degree K of target state information is

$$K = \frac{\left|\left|\max(f_i)\right| - \left|\sum_{i=1}^{M} f_i\right|(f_i)^{-1}\right|}{\left|\max(f_i)\right|} \tag{8}$$

From the above equation, the weights of target state classification are controlled by the weight parameter $c_m(t_i)$ and the clustering degree K. The model enables the data with the same features to complete the clustering, thus realizing the target state recognition. After substituting the clustering degree parameter in formula (8) into the algorithm, the inversion result of formula (5) can be corrected, resulting in more accurate position and angle information, and thus more precise calculation of velocity.

3.2. Target recognition model design

The model constitutes the echo wavelengths with similar attributes into a new input layer by clustering analysis and calculates their corresponding weight parameters. Data mining of the initial wavelength response values is accomplished by clustering analysis, so that the wavelength response information of different types of targets is divided into different data intervals at the input layer. In the data processing layer, the clustering degree is used to filter the wavelength response data containing the state information of the target to be measured, to realize the purpose of improving the accuracy of target recognition. The target recognition model is shown in Fig. 2.

As shown in Fig. 2, the wavelength response signal of FBG is the raw data, in which different FBG positions carry the responsive wavelength information according to different states of the target in the actual test environment. The meaning expressed here by different colors is the difference in wavelength response caused by different types of targets. In (1), the raw wavelength response data are clustered and analyzed. The basis for cluster weights is the duration and amplitude intensity of the response wavelength, as different target states correspond to different durations and intensities. The clustering weights are set concerning Eq. (6). A new collection of separated wavelength response data can be obtained after clustering analysis. This data collection contains

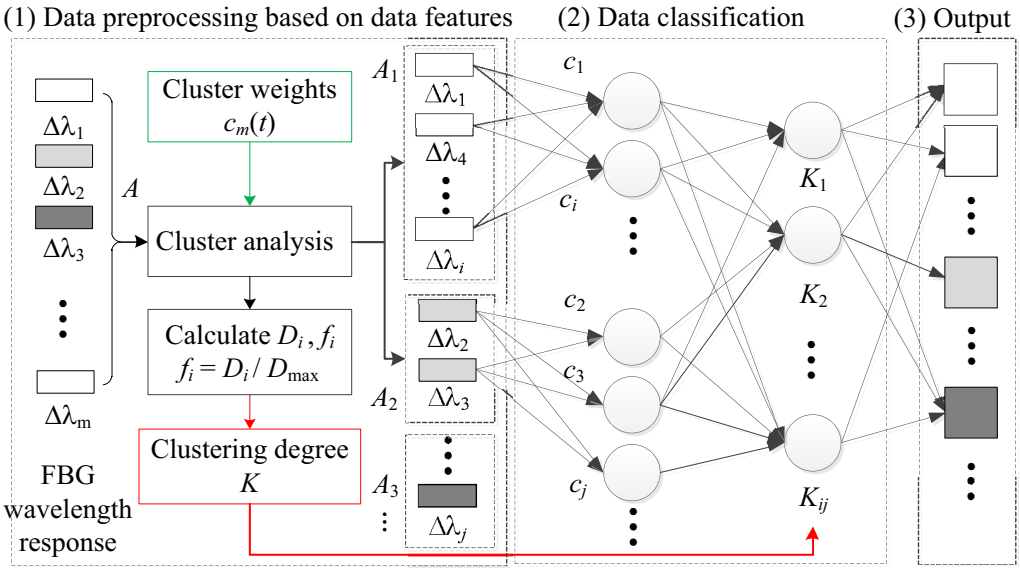

Fig. 2. Target state recognition model based on data mining.

several sub-collections with consistent target state attributes, such as A1 and A2. At the same time, the density metrics containing their state features and their ratio parameters are calculated according to the data features. Finally, the clustering degree of the target state information is obtained. Take the subsets in the new collection as the input data for data classification processing, and take the weight parameter $c_m(t)$ and the clustering degree K as the boundary conditions for data classification. Complete the classification of multi-target state information.

4. Experiments

The target state recognition system based on fiber optic sensing network is shown in Fig. 3. The experiments were carried out using an M1014 broadband light source with a wavelength range of 1525–1565 nm. The demodulator was the THEC-12 fiber optic demodulator with a wavelength resolution of ±1 pm. To simulate the minimum test area in the fiber optic sensing network, nine FBG sensors are selected. The minimum value of the center wavelength is 1526.547 nm, and each bandwidth interval is 3 nm. The test area is an open field of 6.0 m × 6.0 m, and the FBG sensors are laid in a way that is consistent with Fig. 1(a). During the experiment, the system tests three targets simultaneously. Target A: a 75 kg person walking with a mean velocity of 1.0 m/s; target B: a person riding a bicycle (total mass of 85 kg) with a mean velocity of 3.0 m/s; target C: a 65 kg person running with a mean velocity of 4.0 m/s. Because the distribution structure of the whole FBG sensing network is the same, the inversion of the different test results can be performed by discussing only the 2 typical directions of motion calculation. Case 1 is the motion along the *x*-axis, and case 2 is the diagonal

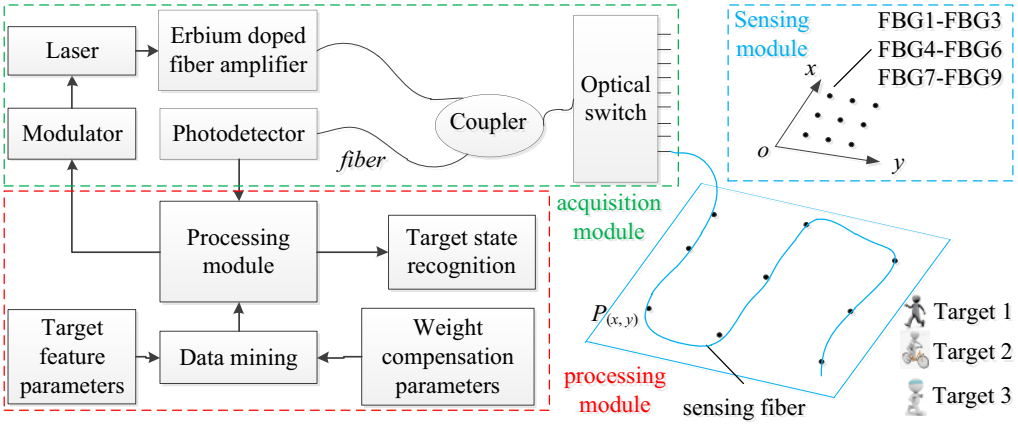

Fig. 3. Target state recognition system based on fiber optic sensing network.

motion along $y = x$. As shown in Fig. 1, the x-axis FBG distribution is equivalent to the y-axis FBG distribution rotated by 90°.

The system mainly consists of three parts: sensing module, acquisition module, and processing module. The sensing module is composed of a fiber optic sensing network, which obtains the vibration signal of the target to be measured in the test area. The testing scope in the testing module is for a minimum unit, and in fact, increasing the testing scope only requires completing the replication of the same testing unit. The acquisition module consists of two parts: output and input. The output is composed of the modulation module, laser, and amplifier to produce the original optical signal. The collection of multiple modules is achieved through time-division multiplexing, and the speed of the time-division multiplexing module is on the order of milliseconds, which can be ignored relative to the test target. The reflected light enters the optical channel to be measured through the coupler and the optical switch, and is transmitted back to the photodetector through the coupler, thereby achieving photoelectric conversion. The electrical signal enters the processing module. Calculate the position and time of the target based on the wavelength response to complete the target state recognition.

4.1. Fiber optic sensing signal acquisition

For a single test target, the intensity of the wavelength response of the FBG can well accomplish the inversion of the target state parameters. When more than one target exists, if two or more targets are in the same FBG sensor in a similar position, it will cause signal overlapping. So it is very important to analyze the recognition probability in the case of overlapping different target motion states. Taking the (1, 1) test position as an example, several signal aliasing waveforms of three targets are tested separately, as shown in Fig. 4.

As shown in Fig. 4(a), the wavelength response quantities are the red curve and blue curve when target A and target B appear separately at the FBG1 position. By the speed difference of their targets, they are highly distinguishable. When the signals are mixed,

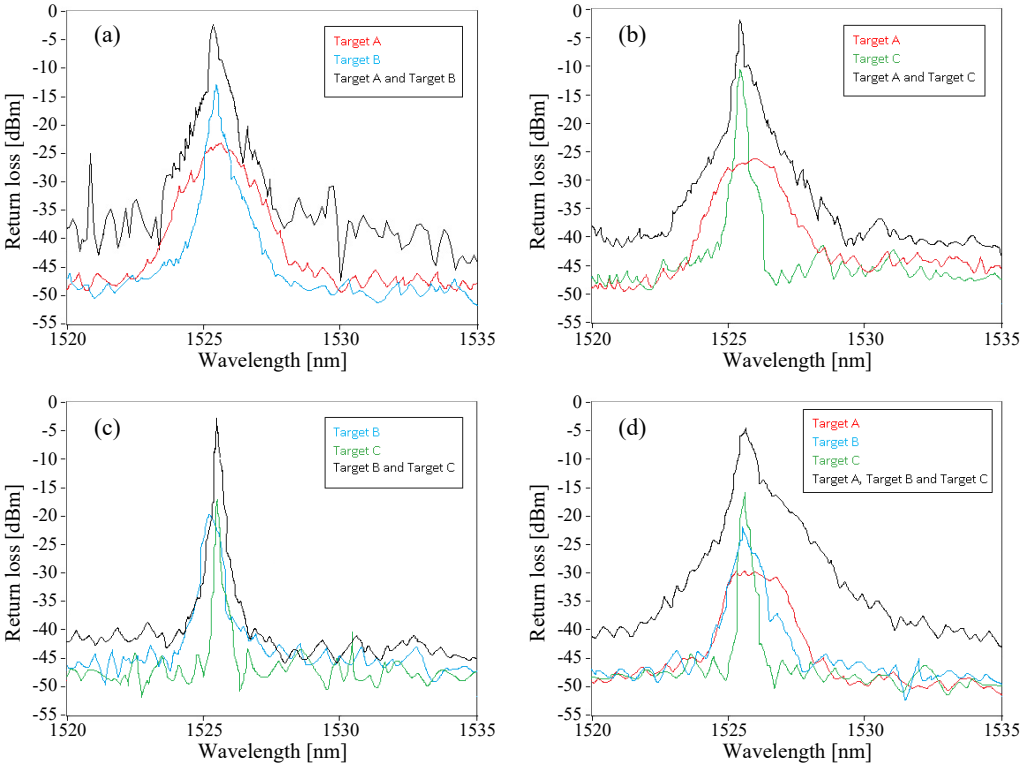

Fig. 4. Wavelength response trend of FBG1 under different target mixing conditions. (a) Target A and target B, (b) target A and target C, (c) target B and target C, and (d) target A, target B and target C.

it is not possible to directly calculate the wavelength response value of each target. However, the system can combine the wavelength response amount of the next FBG sensor that the target passes through to calculate the potential target state information in the overlapped signal. Comparing Figs. 4(a)–(d), the responses of the aliased signals of different targets at the same position have significant differences. When faster-moving targets are present (target C), the narrower the time interval between the locations of the tips of the peaks in the aliased signals. The more targets are aliased, the greater the time width of the overall echo response. According to this pattern of change, the state information of each target in a multi-target system can be calculated more accurately after analyzing the echo signals of different FBGs for data mining. By comparing the width of the echo peak with the amplitude, the type of target can be obtained, so the ratio of half width to amplitude can be used as a distinguishing parameter.

4.2. Multi-target signal recognition analysis

The system sampling frequency is set to 100 Hz to perform smoothing filtering on the echo data, reducing the impact of noise on the test data. This frequency is much higher than the frequency of the test target, thus from the perspective of sampling quantifi-

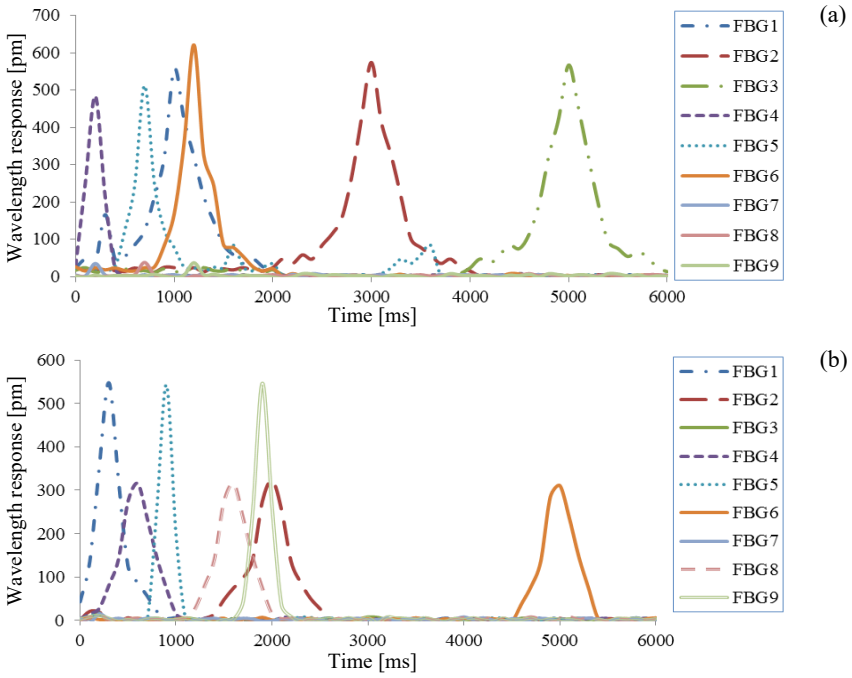

Fig. 5. Response results of FBG sensing network under two motion states. Changes in wavelength response of 9 FBGs over 6 s in (a) case 1, and (b) case 2.

cation this frequency can complete target velocity inversion. Meanwhile, it cannot be too large, otherwise it will increase the difficulty of data processing. Under the conditions of case 1, target A moves from (0, 1) to (6, 1), target B moves from (0, 2) to (6, 2), and C moves from (0, 3) to (6, 3). The test results are shown in Fig. 5(a). Under the condition of case 2, target A moves from (0, 1) to (6, 5), target B moves from (1, 0) to (5, 6), and C moves from (0, 0) to (6, 6). The test results are shown in Fig. 5(b).

As shown in Fig. 5(a), the response times of different FBGs have obvious differences. The response intensity of different FBGs corresponds to the axial distance relationship between the target and FBG. One can calculate the location of the target based on the response intensity of FBG. In the area enclosed by four FBGs in Fig. 1(a), each square area of 1×1 is the minimum position recognition area.

The wavelength shift caused by target A to FBG1, FBG2, and FBG3 is about 550 pm. Its average value of time interval is 2015 ms. The average test speed is 1.99 m/s, with a relative error of 1.3% compared to the true value of 1.0 m/s. Target B shows a superposition state in its response wavelength because it is between FBG1 and FBG3 and between FBG4 and FBG6. The mean value of the wavelength response is 78 pm, and the mean value of the time interval between peaks is 1403 ms. The average test speed is 2.86 m/s, with a relative error of 4.7% compared to the true value of 3.0 m/s. As shown in Fig. 5(b), the wavelength response intensities of FBG2, FBG4, FBG6, and FBG8 are similar because the target C will be directly pressed over FBG1, FBG5, and FBG9.

Therefore, there are peaks and peaks at 315, 925, and 1924 ms. The average test speed is 4.87 m/s, with a relative error of 2.5% compared to the true value of 5.0 m/s. This is determined by the testing of the 2 targets. And the velocity of the three targets can be calculated by the moment of their wavelength response maxima.

4.3. Comparison of recognition probability

After classifying the test data of 9 FBG sensors using data mining under 2 different test conditions, the recognition of three test targets was accomplished. And they were compared with the test data that were not classified and directly subjected to inverse computation, and the probability of target recognition P is shown in Table 1.

T a b l e 1. Comparison of recognition probabilities of targets before and after data mining.

	Data mining	Situation 1				Situation 2			
		A, B	A, C	B, C	A, B, C	A, B	A, C	B, C	A, B, C
P_A [%]	Before	94.3	96.7	0	75.3	91.2	93.7	0	71.5
	After	98.6	99.2	0	93.4	96.3	98.4	0	91.2
P_B [%]	Before	97.1	8.7	65.4	56.2	97.8	13.4	58.4	51.6
	After	99.3	1.9	92.7	90.3	99.1	3.8	88.7	85.7
P_C [%]	Before	0	98.5	74.3	86.1	4.5	97.4	71.2	82.5
	After	0	99.8	94.6	95.8	0.8	99.4	93.1	94.7

The true speed is calculated by moving from a fixed test position to a designated position through a stopwatch. According to the data in Table 1, the recognition probabilities of target A, target B, and target C are all improved to some extent after classification using data mining. When the three targets are mixed, the recognition probability of target A improves from 75.3% to 93.4% at state 1, and it improves from 71.5% to 91.2% at situation 2. The recognition probability of target B improves from 65.4% to 92.7% at state 1. In situation 2, it improves from 51.6% to 85.7%. Its improvement is significant. The recognition probability of target C improves from 86.1% to 95.8% at state 1, and it improves from 82.5% to 94.7% at state 2. For target A, when there are only target B and target C, both test methods are misjudged. However, for targets B and C, there is a certain misjudgment rate, and this algorithm can reduce the target misjudgment rate. Analyzing the distribution of the target recognition rate, it is found that the recognition rate of the aliased signal is lower when the target mass and speed are similar. The closer the test position is to the real position of the FBG sensor, the better its recognition effect is.

5. Conclusions

In response to the signal aliasing problem caused by multiple targets in fiber optic sensing networks, this paper proposes a target state recognition algorithm based on data mining. Based on designing the distribution structure of FBG sensing arrays, a classi-

fication algorithm for targets multi-states recognition based on clustering weights and clustering degree is constructed. Recognition experiments were conducted on two typical target motion states and three types of similar targets. The results demonstrate that after performing data mining on the sensing aliasing signals, the target recognition probability can be effectively improved, and the misjudgment rate can be reduced. The main contribution of this paper is to build a multi-target state inversion model based on fiber optic sensing network data mining. It has certain application value in the field of multi-target state recognition of a fiber optic sensing network.

Funding
This work was supported by *Research on Current Double Closed Loop Control Technology Based on SVPWM Modulation and PR Control*, JJKH20241672KJ.

References

[1] Cramer R., Shaw D., Tulalian R., Angelo P., van Stuijvenberg M., *Detecting and correcting pipeline leaks before they become a big problem*, Marine Technology Society Journal **49**(1), 2015: 31-46. https://doi.org/10.4031/MTSJ.49.1.1

[2] Di Sante R., *Fibre optic sensors for structural health monitoring of aircraft composite structures: Recent advances and applications*, Sensors **15**(8), 2015: 18666-18713. https://doi.org/10.3390/s150818666

[3] Fernández-Ruiz M R, Martins H F, Pastor Graells J, Martin-Lopez S., Gonzalez-Herraez M., *Phase-sensitive OTDR probe pulse shapes robust against modulation-instability fading*, Optics Letters **41**(24), 2016: 5756-5759. https://doi.org/10.1364/OL.41.005756

[4] Tejedor J., Macias-Guarasa J., Martins H.F., Pastor-Graells J., Martín-López S., Guillén P.C., De Pauw G., De Smet F., Postvoll W., Ahlen C.H., González-Herráez M., *Real field deployment of a smart fiber-optic surveillance system for pipeline integrity threat detection: Architectural issues and blind field test results*, Journal of Lightwave Technology **36**(4), 2018: 1052-1062. https://doi.org/10.1109/JLT.2017.2780126

[5] Sidelnikov O., Redyuk A., Sygletos S., *Equalization performance and complexity analysis of dynamic deep neural networks in long haul transmission systems*, Optics Express **26**(25), 2018: 32765-32776. https://doi.org/10.1364/OE.26.032765

[6] Li S., Peng R., Liu Z., Liu X., *Perimeter monitoring of urban buried pipeline threated by construction activities based on distributed fiber optic sensing and real-time object detection*, Optics Express **32**(2), 2024: 2590-2606. https://doi.org/10.1364/OE.509487

[7] Liu Y., Huo X., Liu Z., *Optical fiber network abnormal data detection algorithm based on deep learning*, Infrared and Laser Engineering **50**(6), 2021: 20210029 (in Chinese). https://doi.org/10.3788/IRLA20210029

[8] Geng D., Gong H., *Research on deep mining method of abnormal node data in large-scale optical fiber network*, Laser Journal **44**(4), 2023: 124-128 (in Chinese).

[9] Che L., Ren X., *Anomaly detection algorithm based on sliding windows and confidence for WSN*, Chinese Journal of Sensors and Actuators **36**(11): 1801-1807, 2023 (in Chinese).

[10] Liang Z., Deng K., Ma Y., Wang M., Liu D., Wu H., Wang Y., *An adaptive post-processing algorithm for strain reading anomalies in distributed optical fiber sensors*, Acta Optica Sinica **44**(1), 2024: 0106020 (in Chinese). https://doi.org/10.3788/AOS231457

[11] Pan R., Feng Y., Liu H., Wang H., Zhang H., Zhang Y., Zhang H., *Optical fibre Bragg based sliding-tactile sensing and classification training method for material recognition*, Acta Photonica Sinica **53**(2), 2024: 0206006 (in Chinese). https://doi.org/10.3788/gzxb20245302.0206006

[12] SHANG Q., FAN X., *Fiber optic perimeter security signal recognition method based on CVMD and DBO-SVM*, Semiconductor Optoelectronics **45**(1), 2024: 159-166 (in Chinese).
[13] DU Y.K., SHANG Y., WANG C., YI J.C., SUN M.C., YANG J., ZHAO Y.J., NI J.S., *Intrusive and non-intrusive microflow measurement based on distributed optical fiber acoustic sensing*, Measurement **210**, 2023: 112513. https://doi.org/10.1016/j.measurement.2023.112513

Received May 26, 2025
in revised form July 9, 2025